PROGRESS IN COLOR, COLORANTS AND COATINGS

available online @ www.pccc.icrc.ac.ir

Prog. Color Colorants Coat. 10 (2017), 13-21

Ministry of Science, Research and Technology
Institute for Color Science and Technology

Synthesis of ZnS Decorated Carbon Fibers Nanocomposite and its Application in Photocatalytic Removal of Rhodamine 6G from Aqueous Solutions

A. Mehrizad[*1] and P. Gharbani [2]

[1.] Department of Chemistry, Tabriz Branch, Islamic Azad University, P.O. Box: 5157944533, Tabriz, Iran.

[2.] Department of Chemistry, Ahar Branch, Islamic Azad University, P.O. Box: 5451116714, Ahar, Iran.

ARTICLE INFO

Article history:
Received: 26 Oct 2016
Final Revised: 10 Dec 2016
Accepted: 12 Dec 2016
Available online: 25 Dec 2016

Keywords:
Carbon nanofibers
Photocatalyst
Rhodamine 6G
Zinc sulfide

ABSTRACT

Zinc sulfide/carbon nanofibers (ZnS/CNFs) composite was successfully synthesized through a facile and simple method. X-ray diffraction (XRD) patterns revealed the formation of ZnS decorated CNFs composite. The photocatalytic activity of ZnS/CNFs composite was investigated by the photodegradation of Rhodamine 6G (Rh-6G) dye in aqueous solutions.The effect of operational parameters such as initial Rh-6G concentration, ZnS/CNFs composite concentration, pH and irradiation time were analyzed and optimized by response surface methodology (RSM) in photocatalysis process. The results revealed that the removal percentage of Rh-6G increased with ZnS/CNFs composite concentration, pH and irradiation time, whereas higher initial dye concentration was unfavorable. The findings also showed that under optimum conditions (initial Rh-6G concentration=6 mgL^{-1}, ZnS/CNFs composite concentration= 1.25 g L^{-1}, pH= 8 and irradiation time=48 min) and exposure of UV-C light irradiation (20 Wm^{-2}), the ZnS/CNFs composite exhibited a remarkable photodegradation of Rh-6G dye in aqueous media (99.17%). Prog. Color Colorants Coat. 10 (2017), 13-21© Institute for Color Science and Technology.

1. Introduction

One of the most important environmental pollutants is colored wastewater containing chemicals, which has undesirable effects on human health and other organisms. Regardless of the fact that the presence of such pollutants prevents light infiltration and causes eutrophication phenomenon, it also may cause irreversible threats to human due to carcinogenic, mutagenicity and allergenicity properties [1, 2]. More than ten thousand different synthetic dyes are produced and used for dyeing of fabric annually worldwide. The textile and paint industries are the major colored wastewater producers [3, 4]. Rhodamine 6G (Rh-6G), which is selected as the model compound in this study, is a cationic and basic dye and used widely as a colorant in the manufacturing of textiles and carcinogenic property of this compound has been medically proven [5, 6].

Various strategies such as membrane processes, ion exchange and adsorption have been developed to

*Corresponding author: mehrizad@iaut.ac.ir

remove colored contaminants [7-9]. The drawback of these methods is transfer of pollutants from one phase to another phase rather than eliminating the pollutants from effluent body. In this respect, advanced oxidation processes (AOPs) are well known and widely applied treatment techniques for the complete elimination of textile industries wastewaters [10].

AOPs are based on highly reactive hydroxyl radicals (•OH) generation in sufficient quantity to affect water purification. According to the literature review, semiconductor based photocatalysis are the most popular AOPs in elimination of colored wastewaters. Different semiconductors have been used for this purpose. Due to the non-toxic nature and high negative reduction potential of excited electrons in zinc sulfide (ZnS) owing to its higher conduction band position in aqueous media, ZnS is an appropriate alternative to this purpose [11-13].

In order to increment of the photocatalytic activity, nanosemiconductors can be decorated onto a proper support. Carbonaceous materials such as carbon nanofibers (CNFs) are good hosts for semiconductors in catalytic reactions because of their sufficient stability, extraordinary structural, electrical and mechanical properties and non-toxicity [14].

In this research, ZnS nanoparticles were synthesized via a simple co-precipitation method and afterwards, ZnS decorated CNFs composite was prepared. Modeling and optimization of photocatalytic removal of Rh-6G from aqueous solutions by prepared nanocomposite was conducted using response surface methodology (RSM).

2. Experimental

2.1. Materials

Sodium sulfide flakes (Na_2S) and zinc acetate dihydrate ($Zn(CH_3COO)_2.2H_2O$) were purchased from LobaChemie (India) and Merck (Germany), respectively. CNFs were supplied commercially. Average diameter, pore size and specific surface area of nanofibers were about 130 nm, 0.075 $cm^3\ g^{-1}$ and 24 $m^2\ g^{-1}$, respectively. Rh-6G dye was purchased from S D Fine-Chem limited (India), and its chemical structure is illustrated in Figure 1. Deionized water was used throughout this study.

2.2. Preparation and characterization of ZnS decorated CNFs composite

The ZnS nanoparticles were synthesized by dissolving 0.5 M Na_2S in water. Then, the solution was stirred in a three-neck round-bottom flask under the presence of nitrogen gas. Appropriate amount of zinc acetate solution was slowly added to the above solution and stirred for another 1 h at room temperature. The resulting precipitate was collected by centrifugation and rinsed with ethanol and deionized water for several times.

Afterward, CNFs powder was dispersed in 100 mL of water and sonicated for 15 min. Subsequently, the precipitates coming from the previous stage were added to the CNFs suspension under ultrasonic medium until the uniform precipitate was resulted. The resulting product was finally dried at room temperature and thereafter crushed to obtain fine powder. The prepared ZnS/CNFs composite was characterized in detail by X-ray diffraction (XRD, X'Pert Pro, Panalytical).

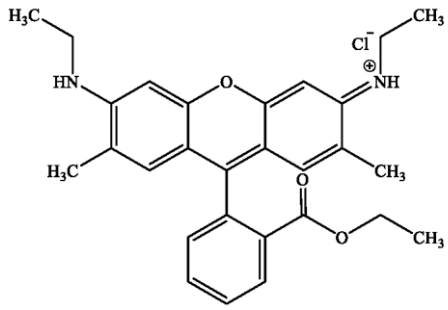

Figure 1: Chemical structure of Rh-6G dye**.**

2.3. Experimental design

Design of experiments (DOE) is a methodical manner to specify the relationship between parameters affecting a process and the output of that process. The focus of the DOE is on the finding a combination of autonomous parameters that optimizes the output of the process.

There are different methods for experimental design among which the RSM is a very fruitful one. RSM is a set of statistical and mathematical approaches to explore the relationships between input and output variables. Central composite design (CCD) is the most generally chosen method in RSM technique.

In this research, Design-Expert 7 (DX7) software was employed for experimental design by RSM based CCD. To evaluate the effect of influenced factors, four operational parameters viz. initial Rh-6G concentration, ZnS/CNFs concentration, pH and irradiation time were chosen and studied in five levels (-α, -1, 0, +1, +α). Values of α can be computed by α = 2k/4, where k is the parameter number. The ranges and the levels of the operational parameters are listed in Table 1.

A total of 30 empirical tests were carried out based on the DX7 software offer, and the obtained data were analyzed. The relationship of mathematical between the operational parameters and response can be explained by the equation (1):

$$y = \beta_0 + \sum_{i=1}^{k} \beta_i x_i + \sum_{i=1}^{k} \beta_{ii} x_i^2 + \sum_{i=1}^{k} \sum_{j=1}^{k} \beta_{ij} x_i x_j + \varepsilon \qquad (1)$$

where y is the process response and β_0 is the constant. β_i, β_{ii} and β_{ij} are coefficients for primary, squared and mutual effects, respectively. x_i and x_j are coded independent variables [15].

2.4. Photocatalytic activity experiments

The photocatalytic properties of the ZnS decorated CNFs composite was evaluated by monitoring the photodegradation of Rh-6G under UV light (20 Wm^{-2}) with respect to the changes of operational parameters. Batch experiments were done in a cylindrical glass reactor containing 100 mL of Rh-6G solution and desired concentration of ZnS/CNFs at a given pH exposed to UV light lamp (Germicidal, China), and the mixture was stirred on a magnetic stirrer. At a regular time intervals, samples were taken, centrifuged and analyzed spectrophotometrically (UV mini-1240, Shimadzu) at absorption peak (525 nm) of Rh-6G. The removal efficiency of Rh-6G was computed by equation (2):

$$R\ (\%) = \left(\frac{A_0 - A_t}{A_0} \right) \times 100 \qquad (2)$$

Where A_0 and A_t are the absorbance of dye when the reaction time is *0* and *t*, respectively.

Table 1: Ranges and levels of the operational parameters.

Parameters	Range and level				
	-α (-2)	**-1**	**0**	**1**	**+α (+2)**
[Rh-6G]$_0$ (mg L^{-1})	2	4	6	8	10
[ZnS/CNFs]$_0$ (g L^{-1})	0.5	0.75	1	1.25	1.5
pH	2	4	6	8	10
Irradiation time (min)	12	24	36	48	60

3. Results and discussion

3.1. Characterization of ZnS decorated CNFs composite

The XRD patterns of CNFs, pristine ZnS, and ZnS/CNFs composite are shown in Figure 2. In original CNFs, the four diffraction peaks at 2θ= 10, 19.5, 21 and 23.5° are characteristic of (020), (110), (120) and (130) planes, respectively. For ZnS, the crystalline peaks appear at 2θ= 28.73, 47.9 and 56.56° indicate the formation of cubic lattice structure of ZnS, which match well with the standard XRD pattern of cubic ZnS [16]. The XRD pattern of the ZnS/CNFs composite includes the characteristic peaks of ZnS with slightly lower crystallinity, which revealed that ZnS nanoparticles are successfully embedded in CNFs matrix.

3.2. Effect of operational parameters

The effect of operational parameters were investigated for evaluation of the photocatalytic activity of the prepared photocatalyst, i.e., ZnS/CNFs composite in the removal of Rh-6G dye. The details of the designed experiments along with the actual and predicted results are given in Table 2.

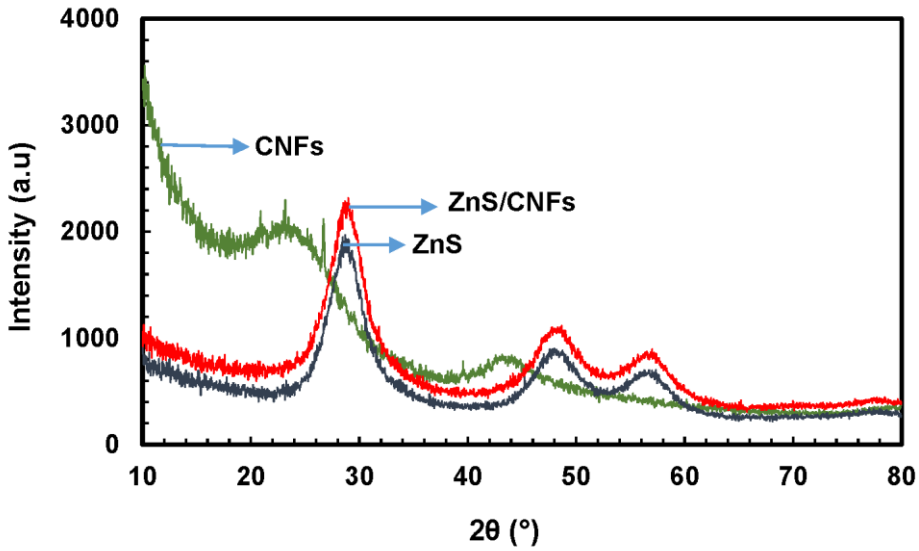

Figure 2: XRD patterns of CNFs, ZnS and ZnS/CNFs.

Table 2: Designed experiments along with actual and predicted results.

Std	Run	Operational parameters				R (%)	
		$[Rh\text{-}6G]_0$ (mg L^{-1})	$[ZnS/CNFs]_0$ (g L^{-1})	pH	Time (min)	Actual	Predicted
1	18	4	0.75	4	24	86.71	83.80
2	8	8	0.75	4	24	51.16	52.61
3	5	4	1.25	4	24	96.46	94.79
4	25	8	1.25	4	24	70.06	71.30
5	20	4	0.75	8	24	83.32	84.44
6	23	8	0.75	8	24	61.13	61.90
7	17	4	1.25	8	24	97.29	98.46

Table 2: Continue.

Std	Run	Operational parameters				R (%)	
		$[Rh\text{-}6G]_0$ (mg L^{-1})	$[ZnS/CNFs]_0$ (g L^{-1})	pH	Time (min)	Actual	Predicted
8	10	8	1.25	8	24	85.80	83.61
9	28	4	0.75	4	48	95.36	96.78
10	14	8	0.75	4	48	90.74	89.83
11	3	4	1.25	4	48	91.60	91.09
12	27	8	1.25	4	48	93.73	91.84
13	6	4	0.75	8	48	96.00	95.01
14	21	8	0.75	8	48	95.79	96.70
15	2	4	1.25	8	48	94.57	92.35
16	13	8	1.25	8	48	98.57	99.73
17	16	2	1	6	36	97.19	99.23
18	12	10	1	6	36	78.96	77.43
19	29	6	0.5	6	36	80.74	80.06
20	4	6	1.5	6	36	94.88	96.08
21	24	6	1	2	36	79.26	80.90
22	1	6	1	10	36	92.56	91.44
23	26	6	1	6	12	68.18	68.43
24	9	6	1	6	60	99.27	99.53
25	7	6	1	6	36	90.06	89.64
26	30	6	1	6	36	88.47	89.64
27	15	6	1	6	36	90.69	89.64
28	11	6	1	6	36	89.85	89.64
29	19	6	1	6	36	90.19	89.64
30	22	6	1	6	36	88.60	89.64

Analysis of variance (ANOVA) was used to study the significance and adequacy of the model (Table 3). The results show a high value of coefficient of determination (Pred*R*-Squared= 0.9837 and Adj *R*-Squared= 0.9685). The Model *F*-value of 64.65 implies that the model is significant. There is only a 0.01% chance that model occurs due to noise. In ANOVA (Table 3), values of "Prob>*F*" which are less than 0.0500 indicate that the model terms are significant. In this case $[Rh\text{-}6G]_0$, $[ZnS/CNFs]_0$, pH, Time, $[Rh\text{-}6G]_0$*$[ZnS/CNFs]_0$, $[Rh\text{-}6G]_0$*pH, $[Rh\text{-}6G]_0$*Time, $[ZnS/CNFs]_0$*Time, pH^2 and $Time^2$ are significant model terms and final reduced equation can be obtained as equation (3):

$$R(\%) = +79.62 - 17.92\left[Rh\text{-}6G\right]_0 + 46.46\left[ZnS/CNFs\right]_0 + 0.07\,pH + 1.38\,Time + 3.85\left[Rh\text{-}6G\right]_0 * \left[ZnS/CNFs\right]_0 + 0.53\left[Rh\text{-}6G\right]_0 * pH + 0.25\left[Rh\text{-}6G\right]_0 * Time - 1.38\left[ZnS/CNFs\right]_0 * Time - 0.21\,pH^2 - 9.82E\text{-}003\,Time^2 \quad (3)$$

Also, residual plots were depicted to evaluate the validity of the selected model. As shown in Figure 3 (a), the inclination of the residuals is towards normal distribution. Figure 3 (b) shows that the residuals in the plot rise and fall randomly around the central line. These two plots revealed that the model is adequate for explaining the process under study.

Table 3: ANOVA for response surface quadratic model.

Source	Sum of squares	Df	Mean square	*F*-value	*p*-value Prob > *F*
Model	3797.59	14	271.26	64.65	< 0.0001
$[Rh\text{-}6G]_0$	712.75	1	712.75	169.86	< 0.0001
$[ZnS/CNFs]_0$	385.20	1	385.20	91.80	< 0.0001
pH	166.69	1	166.69	39.73	< 0.0001
Time	1450.97	1	1450.97	345.80	< 0.0001
[Rh-6G]0*[ZnS/CNFs]0	59.33	1	59.33	14.14	0.0019
[Rh-6G]0*pH	74.61	1	74.61	17.78	0.0007
[Rh-6G]0*Time	587.21	1	587.21	139.95	< 0.0001
[ZnS/CNFs]0*pH	9.17	1	9.17	2.18	0.1601
[ZnS/CNFs]0*Time	278.14	1	278.14	66.29	< 0.0001
pH*Time	5.82	1	5.82	1.39	0.2572
$[Rh\text{-}6G]_0^2$	2.94	1	2.94	0.70	0.4157
$[ZnS/CNFs]_0^2$	4.25	1	4.25	1.01	0.3302
pH^2	20.70	1	20.70	4.93	0.0422
$Time^2$	54.91	1	54.91	13.09	0.0025
Residual	62.94	15	4.20		
Lack of Fit	58.86	10	5.89	7.22	0.0207
Pred *R*-Squared: 0.9837		Adj *R*-Squared: 0.9685			

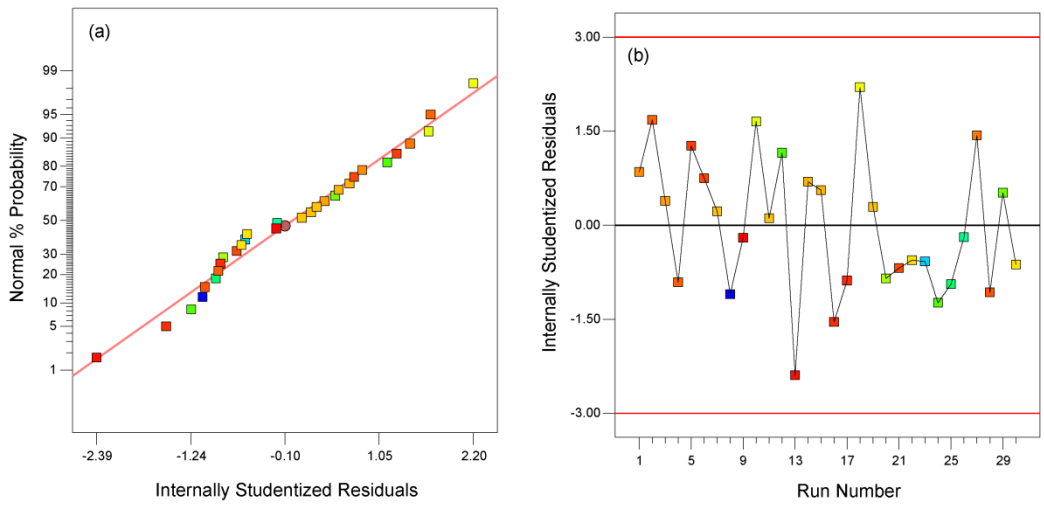

Figure 3:(a) Normal plot of residuals; (b) Residuals versus run number.

In continuation of our investigations, counter plots were depicted with two parameters kept constant at their zero level and the other two varying within the experimental ranges. It is obvious from Figure 4 (a)-(f) that the removal percentage of Rh-6G increased with ZnS/CNFs concentration, pH and irradiation time, whereas higher initial dye concentration was unfavorable.

In fact, increasing the amount of photocatalyst leads to an increase of available catalytic and adsorption sites on the ZnS/CNFs surface, which are effective for increment of photocatalytic activity. On the other hand, hydroxyl radicals' production increases with the amount of photocatalyst [17]. Similar result was presented for removal of Methylene Blue from aqueous solution using nano-TiO_2/UV process [10].

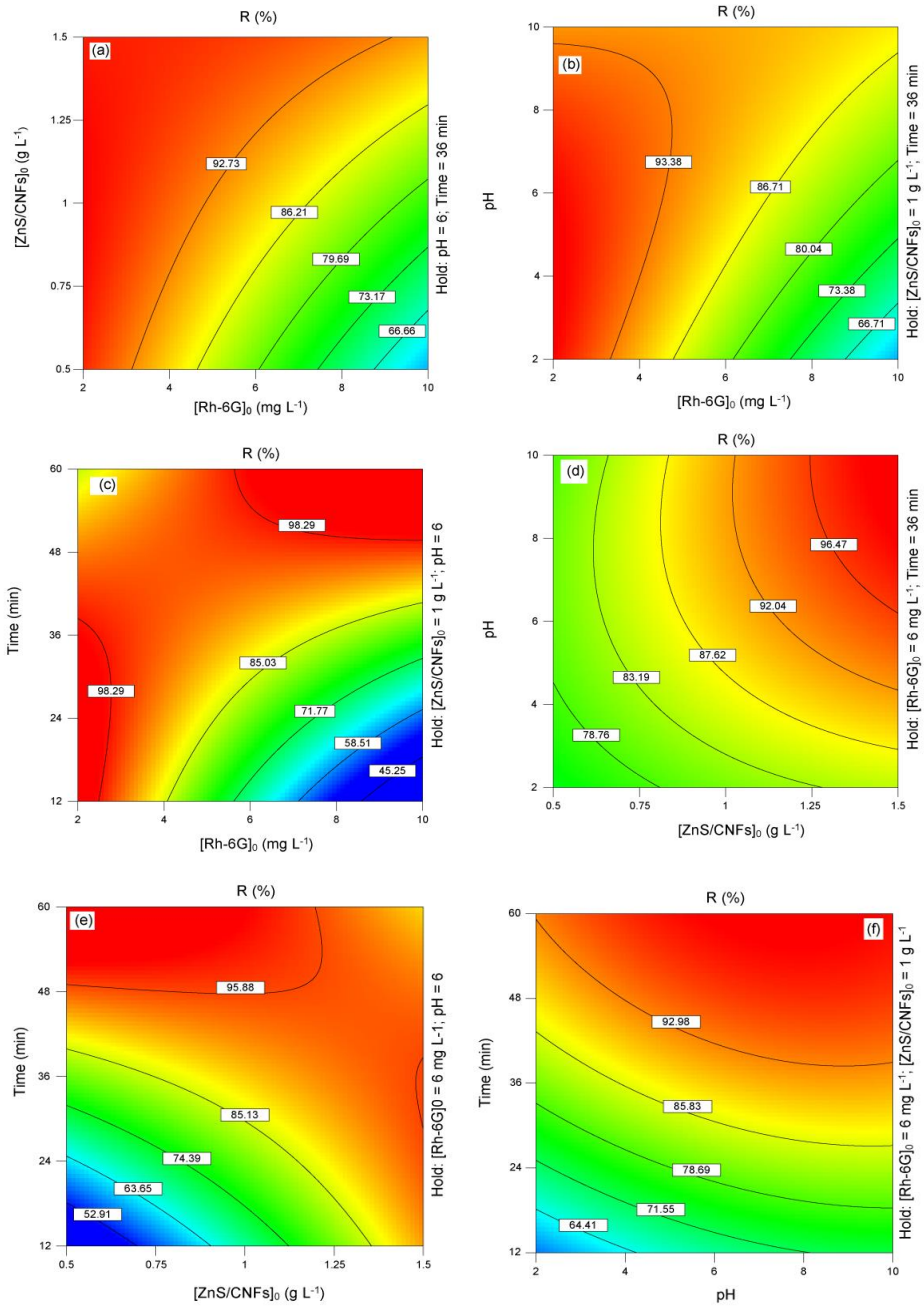

Figure 4: Counter plots of removal efficiency (%) as a function of (a) initial Rh-6G concentration and ZnS/CNFs concentration; (b) initial Rh-6G concentration and pH; (c) initial Rh-6G concentration and irradiation time; (d) ZnS/CNFs concentration and pH; (e) ZnS/CNFs concentration and irradiation time; (f) pH and irradiation time

Also, it can be seen that the removal efficiency of dye was improved with increasing of pH. The presumed reason is that since the pH of isoelectric point for ZnS/CNFs is about 7 (data not shown here), a strong electrostatic adsorption of the Rh-6G cationic dye on the ZnS/CNFs surface at alkaline pH values led to intensification in photodegradation. On the other hand, at alkaline pH values, hydroxyl radicals generated by the photocatalytic process gradually increase and cause destruction of organic compounds such as dye molecules.This results are consistent with the findings of other researches [18, 19].

According to counter plots, increasing the initial concentration of Rh-6G reduces the removal efficiency. Indeed, by increasing the Rh-6G concentration, the amount of light penetrating into the dye solution to reach the catalyst surface is reduced and as such, the production of reactive hydroxyl and superoxide radicals is reduced [20]. Similar results were reported for the photocatalytic degradation of Basic Red 46 dye and leather dye on TiO_2 [21, 22].

As is clear from Figure 4, increasing the duration of UV radiation has a positive effect on the removal efficiency of dye. Actually, the generation of conduction band electron-valence band hole pairs ($e^-_{CB}+h^+_{VB}$) and consequently production of hydroxyl radicals increased with irradiation time and more attack of hydroxyl radicals lead to higher dye removal amount [23]. Finally, based on the results of the optimization process by CCD, under optimum condition (initial Rh-6G concentration= 6 mg L-1, ZnS/CNFs composite concentration= 1.25 g L-1, pH= 8 and irradiation time= 48 min), dye removal efficiency reached to 99.17%. This was verified experimentally (98.21%) and is further evidenced from the success of the designed model.

4. Conclusions

ZnS nanoparticles were decorated on CNFs by a simple method and prepared nanocomposite was characterized by XRD patterns. The photocatalytic removal behavior of Rh-6G by ZnS/CNFs composite under UV-C light irradiation was investigated by RSM. The experimental and model predicted values were compared and it was found that predicted values by RSM were in reasonable agreement with experimental results (R^2= 0.9837). Based on the results, the removal percentage of Rh-6G increased with increasing ZnS/CNFs concentration, pH and irradiation time, whereas higher initial dye concentration was unfavorable. The findings also showed that under optimal condition, dye removal efficiency reached to 99.17% that was also verified experimentally (98.21%).

Acknowledgements

The authors would like to thank Tabriz Branch, Islamic Azad University for the financial support of this research, which is based on a research project contract.

5. References

1. A.Y. Zahrim, C. Tizaoui, N. Hilal, Coagulation with polymers for nanofiltration pre-treatment of highly concentrated dyes: A review, *Desalination*, 266(2011), 1-16.
2. G. Ciobanu, M. Harja, L. Rusu, A. Mihaela Mocanu, Acid Black 172 dye adsorption from aqueous solution by hydroxyapatite as low- cost adsorbent, *Korean J. Chem. Eng.*, 31(2014), 1021-1027.
3. M.J. Mughal, R. Saeed, M. Naeem, M.A. Ahmed, A. Yasmien, Q. Siddiqui, M. Iqbal, Dye fixation and decolourization of vinyl sulphone reactive dyes by using dicyanidiamide fixer in the presence of ferric chloride, *J. Saudi chem. Soc.*, 17(2013), 23-28.
4. A. Mohammadi, A. Aliakbarzadeh Karimi, H. Fallah Moafi, Adsorption and photocatalytic properties of surface-modified TiO_2 nanoparticles for Methyl Orange removal from aqueous solutions, *Prog. Color Colorants Coat.*, 9(2016), 247-258.
5. A. Vanamudan, P. Pamidimukkala, Chitosan, nanoclay and chitosan–nanoclay composite as adsorbents for Rhodamine-6G and the resulting optical properties, *Int. J. Biol. Macromolec.*, 74(2015), 127–135.
6. S. Rajoriya, S. Bargole, V.K. Saharan, Degradation of a cationic dye (Rhodamine 6G) using hydrodynamic cavitation coupled with other oxidative agents: Reaction mechanism and pathway, *Ultrason. Sonochem.*, 34(2017), 183-194.
7. R. Gopal, S. Kaur, Z. Ma, C. Chan, S. Ramakrishna, T. Matsuura, Electrospun nanofibrous filtration membrane, *J. Membrane Sci.*, 281(2006), 581–586.
8. M. Imran Khan, S. Akhtar, S. Zafar, A. Shaheen, M. Ali Khan, R. Luque, A. Ur Rehman, Removal of Congo Red from aqueous solution by anion exchange membrane (EBTAC): Adsorption kinetics and themodynamics, *Materials*, 8(2015), 4147-4161.

9. M. T. Yagub, T. K. Sen, S. Afroze, H. M. Ang, Dye and its removal from aqueous solution by adsorption: a review, *Adv. Colloid Interface Sci.*, 209(2014), 172-84.
10. A. Mehrizad, P. Gharbani, Removal of Methylene blue from aqueous solution using nano-TiO_2/UV Process: Optimization by response surface methodology, *Prog. Color Colorants Coat.*, 9(2016), 135-143.
11. A. Di Paola, E. Garcia-Lopez, G. Marci, L. Palmisano, A survey of photocatalytic materials for environmental remediation, *J. Hazard. Mater.*, 211(2012), 3-29.
12. J. Kaur, M. Sharma, O.P. Pandey, Structural and optical studies of undoped and copper doped zinc sulphide nanoparticles for photocatalytic application, *Superlattice. Microst.*, 77(2015), 35-53.
13. L. Yin, D. Zhang, D. Wang, X. Kong, J. Huang, F. Wang, Y. Wu, Size dependent photocatalytic activity of ZnS nanostructures prepared by a facile precipitation method, *Mat. Sci. Eng. B*, 208(2016), 15-21.
14. A. Mehrizad, P. Gharbani, Study of 1-chloro-4-nitrobenzene adsorption on carbon nanofibers by experimental design, *Int. J. Nano Dimens.*, 7(2016), 77-84.
15. M. Almeida Bezerra, R. Erthal Santelli, E. Padua Oliveira, L. Silveira Villar, L. Amelia Escaleira, Response surface methodology (RSM) as a tool for optimization in analytical chemistry, *Talanta*, 76(2008), 965–977.
16. A. Guinier, X-ray Diffraction in crystals, Imperfect crystals, and amorphous, X-ray Diffraction, Freeman, San Francisco, 1963.
17. D. Gumus, F. Akbal, Photocatalytic degradation of textile dye and wastewater, *Water Air Soil Pollut.*, 216(2011), 117-124.
18. A. Olad, R. Nosrati, Preparation, characterization, and photocatalytic activity of polyaniline/ZnO nanocomposite, *Res. Chem. Intermed.*, 38(2012), 323–336.
19. R. Nagaraja, N. Kottam, C.R. Girija, B.M. Nagabhushana, Photocatalytic degradation of Rhodamine B dye under UV/solar light using ZnO nanopowder synthesized by solution combustion route, *Powder Technol.*, 215-216(2012), 91-97.
20. H.R. Rajabi, O. Khani, M. Shamsipur, V. Vatanpour, High-performance pure and Fe^{3+}-ion doped ZnS quantum dots as green nanophotocatalysts for the removal of malachite green under UV-light irradiation, *J. Hazard. Mater.*, 250– 251(2013) 370–378.
21. L.C. Macedo, D.A.M. Zaia, G.J. Moore, H. de Santana, Degradation of leather dye on TiO_2: A study of applied experimental parameters on photoelectrocatalysis, *J. Photochem. Photobiol.*, 185(2007), 86-93.
22. M. Zarei, A.R. Khataee, R. Ordikhani-Seyedlar, M. Fathinia, Photoelectro Fenton combined with photocatalytic process for degradation of an azo dye using supported TiO_2 nanoparticles and carbon nanotube cathode: Neural network modeling, *Electrochim. Acta*, 55(2010), 7259-7265.
23. N. Ertugay, F. Nuran Acar, The degradation of Direct Blue 71 by sono, photo and sonophotocatalytic oxidation in the presence of ZnO nanocatalyst, *Appl. Surf. Sci.*, 318(2014), 121-126.

How to cite this article:
A. Mehrizad and P. Gharbani, Synthesis of ZnS decorated carbon fibers nanocomposite and its application in photocatalytic removal of Rhodamine 6G from aqueous solutions, Prog. Color Colorants Coat., 10 (2017), 13-21.